Electron-spin resonance of uv-irradiated sodium azide*

Ralph H. Bartram, Lawrence A. Kappers, and Gary G. DeLeo
Physics Department and Institute of Materials Science, University of Connecticut, Storrs, Connecticut 06268
(Received 19 July 1976)

Electron-spin-resonance (ESR) spectra were measured on NaN_3 single crystals, uv irradiated at 77 K, and correlated with the optical-absorption spectra described in the preceding paper. A new ESR spectrum is observed, corresponding to spin $S = 1$ in three inequivalent sites. The growth and decay of the spin-1 spectrum correlate, respectively, with the fast and slow annealing stages of the 565-nm optical absorption band, which occur below and above 220 K. The 565-nm band is attributed to spin-1/2 defects which form antiferromagnetically exchange-coupled pairs, and several models for these defects are considered. The 19-line *F*-center ESR spectrum correlates only with the less-stable component of the 735-nm band. The prominent single ESR line which remains after annealing of the 19-line spectrum is not correlated with the 610-nm band, contrary to previous reports.

I. INTRODUCTION

The crystal structure and properties of NaN_3 were described in the previous paper.[1] The electron-spin-resonance (ESR) spectra of radiation-induced defects in NaN_3 were investigated by Miller and co-workers at Fort Belvoir, Va.,[2-8] and by Gelerinter and Silsbee.[9-11] Miller and co-workers correlated a 19-line ESR spectrum in uv-irradiated NaN_3, which they attributed to the *F* center, with an optical-absorption band at 735 nm.[4,6] They also reported a single ESR line, which remains after the *F* center is annealed. On the basis of its annealing behavior at room temperature, they correlated this ESR line with a 610-nm optical-absorption band which they attributed to the F_2^+ center.[6]

These correlations are reexamined in the present work. In addition, three new ESR spectra are reported. These include a six-line spectrum, produced by uv irradiation at 77 K and subsequent thermal treatment, whose relation to the optical spectra reported in the previous paper[1] is discussed.

Experimental procedures are described in Sec. II, and results presented in Sec. III. Possible interpretations of the defect structure are considered in Sec. IV.

II. EXPERIMENTAL PROCEDURES

ESR measurements were made on both the relatively thick single crystals of NaN_3 used for optical measurements[1] and thinner crystals grown by O. R. Gilliam at the University of Connecticut, with equivalent results. The crystals were mounted, either flat or on edge, on the end of a brass rod, and were uv irradiated at 77 K. They were subsequently transferred to the microwave cavity of a Varian E-3 ESR spectrometer without appreciable warming. Pulsed-annealing experiments were performed with the variable-temperature accessory. The annealing procedure followed was similar to that for the optical measurements described in the previous paper,[1] except that ESR measurements were made at 90 K rather than 77 K. In addition, some measurements were made at 4.2 K with a Varian E-12 ESR spectrometer.

III. EXPERIMENTAL RESULTS

After uv irradiation at 77 K, single crystals of NaN_3 were subjected to a series of isochronal pulsed anneals, each for 5 min, at 20-K intervals between 100 and 280 K. The ESR spectra were measured at 90 K after each anneal. Several distinct ESR spectra produced in this manner are described below.

The most prominent spectrum observed after uv irradiation is the 19-line spectrum which was described by Carlson *et al.*[4] who attributed it to the *F* center. This spectrum is observed to anneal between 100 and 180 K, as shown in Fig. 1. This figure also shows the difference between the optical density of the 735-nm band at each temperature and that at 180 K; i.e., it shows the annealing of the less-stable component of the 735-nm band. It can be seen from Fig. 1 that this component of the 735-nm band correlates very well with the 19-line spectrum, in confirmation of the conclusion reported previously by King *et al.*[6]

The ESR spectrum which remains after the 19-line spectrum has annealed is shown in Fig. 2 for $\vec{H}$ parallel to the hexagonal *c* axis. This spectrum is apparently present at 77 K, but is obscured by the 19-line spectrum.[5] The three distinct lines evident in this spectrum are found to be associated with three different defects, and will be described separately.

The most prominent of these lines, with a width of 15 G, has essentially axial symmetry about the

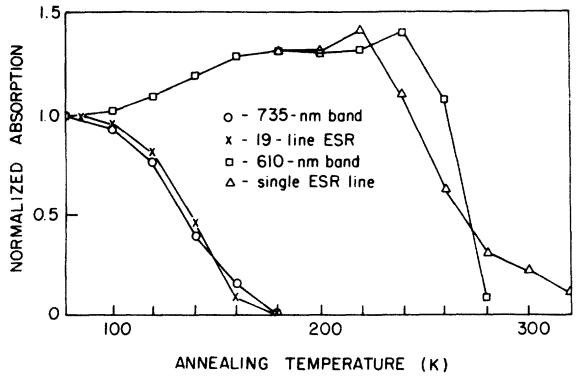

FIG. 1. Intensities of the 19-line F-center ESR spectrum and the prominent single ESR line of Fig. 2 are compared, respectively, with the relative optical densities of the 735-nm band and the 610-nm band as functions of annealing temperature for 5-min isochronal pulsed anneals. The optical density of the 735-nm band for 180 K was subtracted from the values for lower annealing temperatures, and the difference was normalized to unity at 77 K. The 19-line ESR spectrum and the 610-nm band were also normalized to unity at 77 K, while the single ESR line was matched to the 610-nm band at 180 K.

c axis with the g values listed in Table I. The annealing behavior of the prominent single line was studied by first warming a uv-irradiated NaN_3 crystal directly to 180 K for 10 min in order to eliminate the 19-line spectrum, and by subsequently subjecting the crystal to 5-min isochronal pulsed anneals at 20-K intervals between 180 and 280 K. The intensity of the ESR line is compared with the optical density of the 610-nm band as a function of

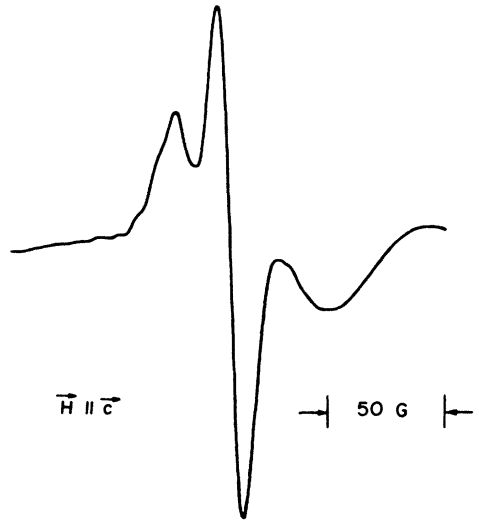

FIG. 2. ESR spectrum of uv-irradiated NaN_3 for $\vec{H}$ parallel to the c axis, after warming to 180 K to remove the 19-line spectrum.

TABLE I. Spin-Hamiltonian parameters for $S=\frac{1}{2}$ ESR spectra. These spectra have axial symmetry about the hexagonal c axis.

	Prominent line	Broad line
$g_{\parallel}$	1.989 ± 0.001	1.97 ± 0.01
$g_{\perp}$	2.005 ± 0.001	2.00 ± 0.01

annealing temperature in Fig. 1. It is apparent from Fig. 1 that the annealing of the single ESR line does *not* correlate in detail with that of the 610-nm band, contrary to the conclusion of King *et al.*,[6] although both anneal in roughly the same temperature range. This observation was corroborated by further measurements which showed that the 610-nm band anneals much more rapidly than the single ESR line at 270 K. Furthermore, room-temperature x-ray irradiation was found to generate the single ESR line without the 610-nm band.

The set of isochronal pulsed anneals above 180 K, employed in studying the annealing behavior of the prominent single ESR line, also revealed a new ESR spectrum, corresponding to a center with spin $S=1$ in three inequivalent sites. This spectrum is shown in Fig. 3, together with the single ESR line, for orientation of the magnetic field parallel to the hexagonal c axis. The spin-one spectrum appears as the two outer lines in Fig. 3, with peak-to-peak linewidth of 25 G, and breaks up into six lines at other magnetic field orientations. Spectra were recorded at 2° intervals on x-ray-oriented samples, and spin-Hamiltonian parameters were obtained by a least-squares fit to a spin Hamiltonian of the form

$$\mathcal{H}_S = \mu_B[g_{\parallel}H_{z'}S_{z'} + g_{\perp}(H_{x'}S_{x'} + H_{y'}S_{y'})] + D[S_{z'}^2 - \tfrac{1}{3}S(S+1)]. \quad (1)$$

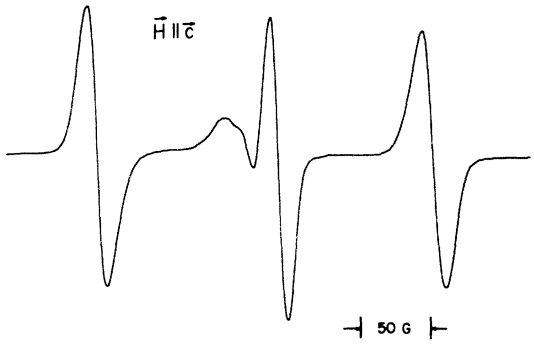

FIG. 3. ESR spectum of uv-irradiated NaN_3 for $\vec{H}$ parallel to the c axis, after warming to 220 K. The two outer lines constitute the spin-1 spectrum. The prominent central line is identical with that shown in Fig. 2.

TABLE II. Spin-Hamiltonian parameters for $S=1$ ESR spectra associated with three inequivalent sites. Polar angles θ' and ϕ' refer to the orientation of the unique principal axis of the $\vec{g}$ tensor, while angles θ and ϕ give the orientation of the effective crystal field (pair axis).

	Site 1	Sites 2 and 3
$g_{\parallel}$	1.9917 ± 0.001	1.9913 ± 0.001
$g_{\perp}$	2.0038 ± 0.001	2.0023 ± 0.001
θ'	$5 \pm 3°$	$15 \pm 3°$
ϕ'	0°	0°
D (G)	178 ± 2	197 ± 2
θ	$27° \pm 1°$	$31° \pm 1°$
ϕ	0°	$\pm(121° \pm 1°)$

The spectrum corresponding to each site appears to have nearly axial symmetry about an axis tilted approximately 30° with respect to the c axis; the symmetry axes for the three sites are separated in azimuth by approximately 120° and are nearly parallel to edges of the rhombohedral unit cell shown in Fig. 1 of Ref. 1. However, the principal axis for $g_{\parallel}$ does not coincide with that for the zero-field splitting parameter D. The optimum spin-Hamiltonian parameters and precise principal axis orientations for the three sites are listed in Table II. The angular variation of the magnetic field required for resonance, calculated from these parameters, is compared with experiment in Fig. 4. It should be observed in connection with these data that two types of twinning can occur in NaN_3: One type is present in the rhombohedral phase, and can be described as a rotation of one crystal with respect to another by 30° about the c axis. The second type appears only in the monoclinic phase;

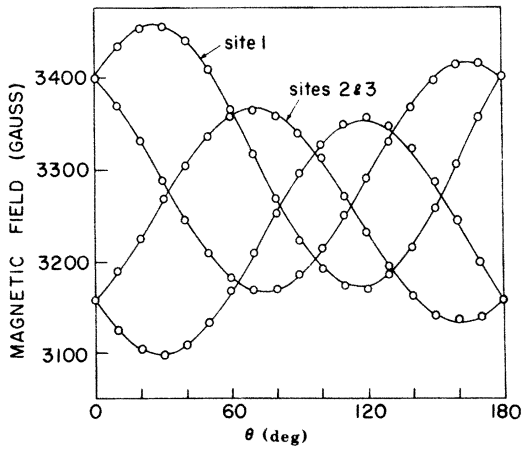

FIG. 4. Angular dependence of the spin-1 ESR-spectrum, calculated from the spin-Hamiltonian parameters of Table II. The data are shown as circles. The field required for resonance is shown as a function of polar angle θ, for $\vec{H}$ in the yz plane of Fig. 1 of Ref. 1.

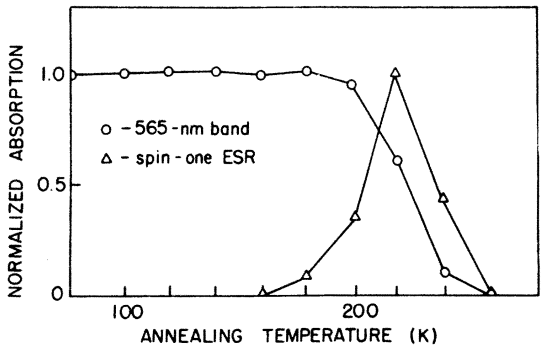

FIG. 5. Intensity of the spin-1 ESR spectrum and relative optical density of the 565-nm band as a function of annealing temperature for 5-min isochronal pulsed anneals. The 565-nm band is normalized to unity at 77 K, and the ESR line at 220 K.

there are three possible orientations of the monoclinic b axis perpendicular to the c axis (see Fig. 2 of Ref. 1), and different orientations can occur in successive layers perpendicular to the c axis. The data shown in Fig. 4 correspond to a single monoclinic crystal whose b axis is perpendicular to the plane of the magnetic field. Much weaker ESR

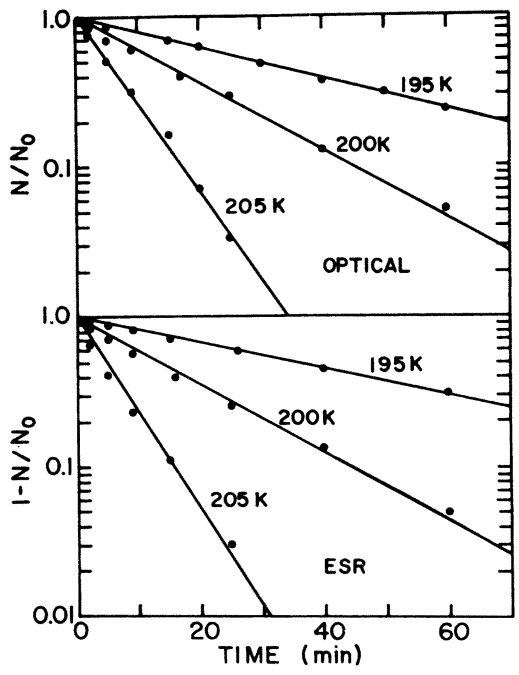

FIG. 6. Fast annealing stage of the 565-nm band and growth of the spin-1 ESR spectrum. (a) The difference between the optical density of the 565-nm band and its asymptotic value as a function of time for several discrete temperatures. (b) The difference between the asymptotic intensity of the spin-1 ESR spectrum and its intensity at time t for several discrete temperatures. Both curves are normalized to unity at $t=0$.

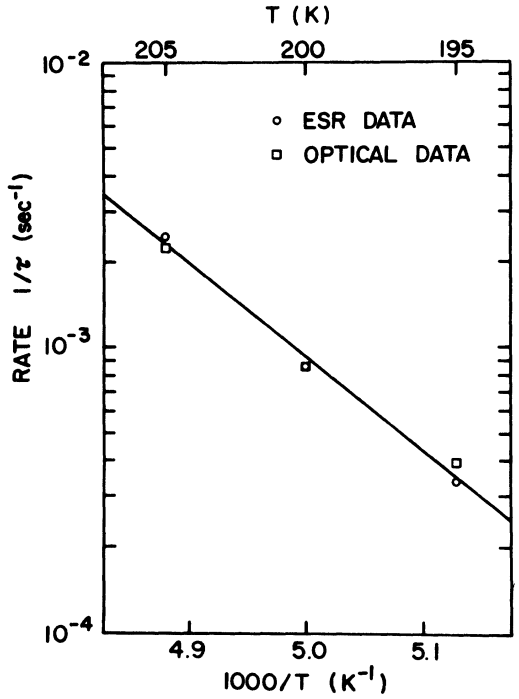

FIG. 7. Fast annealing rate for the 565-nm band and growth rate for the spin-1 ESR spectrum as a function of temperature. Each datum point corresponds to one curve of Fig. 6. The activation energy and frequency factor derived from the slope and intercept of this curve are listed in Table III.

spectra corresponding to both types of twins were also observed.

The dependence of the intensity of the spin-1 spectrum on annealing temperature is shown in Fig. 5, where it is compared with the optical density of the 565-nm band. It is evident that the two spectra are related in a complex way. The temperature dependence of the spin-1 spectrum was investigated further by measuring its intensity as a function of time at several fixed temperatures. It was found that the growth and annealing of this spectrum are sufficiently well-separated in temperature to be studied independently, and that they correlate respectively with fast and slow annealing stages of the 565-nm band.[1] The growth and annealing data for the ESR spectrum are summarized and compared with optical annealing data in Figs. 6–9, from which it is evident that both stages follow first-order kinetics. The rapid annealing of the 565-nm band is exponential in time, while the growth of the spin-1 ESR spectrum is a saturating exponential. Both processes are characterized by the same rate constant α, which has temperature dependence of the form,

$$\alpha = se^{-E/kT}, \tag{2}$$

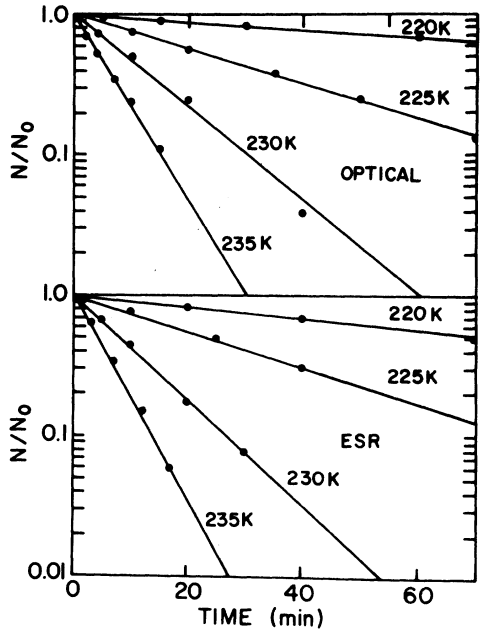

FIG. 8. Slow annealing stage of the 565-nm band and annealing of the spin-1 ESR spectrum. (a) Relative optical density of the 565-nm band as a function of time for several discrete temperatures. (b) Relative intensity of the spin-1 ESR signal as a function of time for several discrete temperatures.

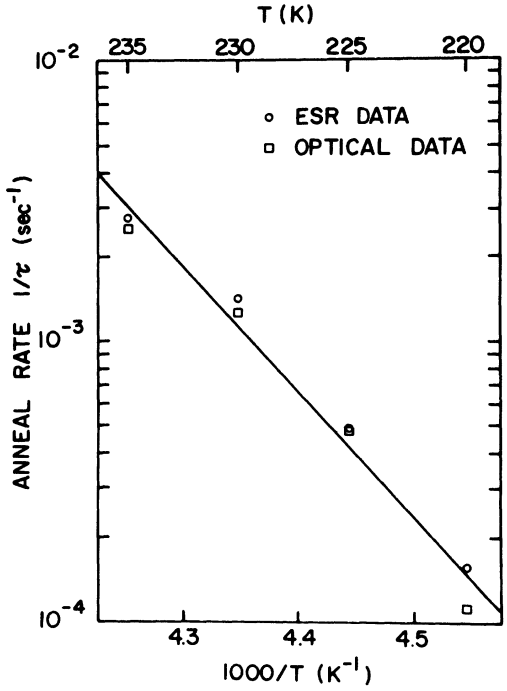

FIG. 9. Slow annealing rate for the 565-nm band and annealing rate for the spin-1 ESR spectrum as a function of temperature. Each datum point corresponds to one curve of Fig. 8. The activation energy and frequency factor derived from the slope and intercept of this curve are listed in Table III.

with frequency factor s and activation energy E. Approximately 25% of the 565-nm band anneals in the fast stage. The fast annealing stage is accompanied by a slight but discernable qualitative change in the residual band, which is broadened from 0.46 to 0.49 eV and shifted slightly to shorter wavelength as shown in Fig. 10. The slow annealing of this residual band is accompanied by annealing of the spin-1 spectrum. Both processes have exponential time dependence characterized by the same rate constant, again with the temperature dependence of Eq. (2). Activation energies and frequency factors for the fast and slow processes are listed in Table III. The association of the spin-1 spectrum with the 565-nm band is well established by these data.

The intensity of the spin-1 spectrum was measured at 4.2 K, and was found to be smaller by a factor of 10 than would be expected on the basis of its intensity at 77 K. It was established that this effect is reversible, and is not due to power saturation.

The relatively weak, broad single line on the high-field side in Fig. 2, of width 40 G, grows nonlinearly with dose, being relatively more intense in heavily irradiated samples. It has axial symmetry about the c axis, with g values listed in Table I. The time dependence of annealing of this broad line was measured at 200 K, and was found to be correlated with the rapid annealing stage of the 565-nm band and the growth of the spin-1 spectrum.

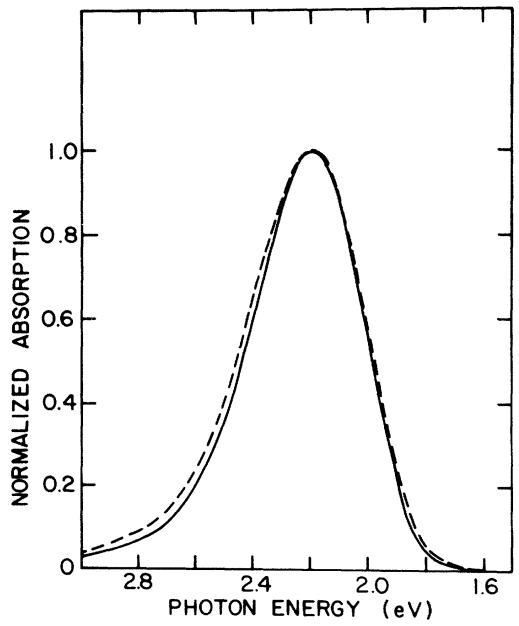

FIG. 10. 565-nm band. (a) Solid curve: before the fast annealing stage and (b) dashed curve: after the fast annealing stage.

TABLE III. Activation energies and frequency factors for the growth and decay of the spin-1 ESR spectrum, which correlate, respectively, with the fast and slow annealing stages of the 565-nm band. These data are derived from Figs. 7 and 9.

	Growth of $S=1$ and fast stage	Decay of $S=1$ and slow stage
E (eV)	0.64 ± 0.05	0.90 ± 0.05
s ($\sec^{-1}$)	1×10^{13}	5×10^{16}

The weak narrow band which appears as a shoulder on the low-field side of the prominent single line in Fig. 2 is part of a spectrum with a highly anisotropic $\tilde{g}$ tensor which reveals a resolved five-line hyperfine structure in some orientations. This spectrum is relatively persistent in annealing, and is still apparent after warming briefly to room temperature. The angular variation of this spectrum is difficult to follow in uv-irradiated NaN_3. The same spectrum has been observed much more clearly in x-ray-irradiated NaN_3,[12] and will be described in a separate publication.

IV. DISCUSSION

In the absence of resolved hyperfine structure, it is not possible to make a positive identification of the defect responsible for the spin-1 ESR spectrum. However, the available evidence points strongly to the conclusion that this spectrum arises from exchange-coupled pairs of spin-$\frac{1}{2}$ defects. According to Table II, the axes for the zero-field splitting parameter D are oriented approximately parallel to primitive lattice vectors (the edges of the rhombohedral unit cell in Fig. 1 of Ref. 1), while the principal axes corresponding to $g_{\|}$ are all tilted in one direction in the crystal, the same direction in which the azide ions are tilted by monoclinic distortion.[13] These geometrical relations suggest that the spin-$\frac{1}{2}$ defects occupy equivalent sites in contiguous unit cells; see Fig. 11. The spin-Hamiltonian for exchange-coupled pairs is[14]

$$\mathcal{H} = J\vec{S}_1 \cdot \vec{S}_2 + \mu_B \vec{H} \cdot \tilde{g} \cdot (\vec{S}_1 + \vec{S}_2) + D_d(3S_{z1}S_{z2} - \vec{S}_1 \cdot \vec{S}_2), \quad (3)$$

where the terms on the right-hand side, listed in descending order, are the isotropic exchange interaction, the Zeeman interaction, and the dipolar interaction. (The latter may also include a contribution due to anisotropic exchange, which we will neglect.) The isotropic exchange interaction alone is diagonal in the coupled representation, yielding

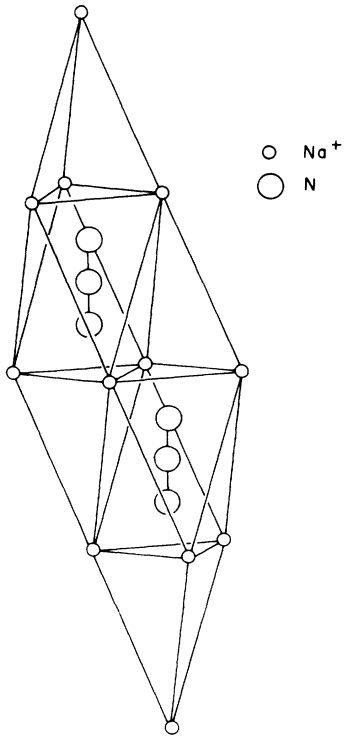

FIG. 11. Model for the spin-1 spectrum of Figs. 3 and 4: exchange-coupled pairs of spin-$\frac{1}{2}$ defects which substitute for the azide ions shown.

unperturbed energies

$$E_0(S) = \tfrac{1}{2}J[S(S+1) - \tfrac{3}{2}], \tag{4}$$

and the remaining terms can be represented within the triplet manifold in the form of Eq. (1), with

$$D = \tfrac{3}{2}D_{\alpha} = -\tfrac{3}{2}(g^2\mu_B^2/r_{12}^3). \tag{5}$$

The small anisotropy of g has been neglected in Eq. (5). If we assume that the separation of spin-$\frac{1}{2}$ defects equals the rhombohedral unit cell edge length 5.488 Å, Eq. (5) yields $D = -168$ G, in good agreement with the values listed in Table II.

The diminished intensity of the spin-1 spectrum at 4.2 K reveals that the exchange interaction is antiferromagnetic; i.e., the $S = 1$ states lie above the $S = 0$ state and are thermally populated. The relative population of one component of the $S = 1$ manifold is given by[14]

$$I_1 = e^{-J/kT}/(1 + 3e^{-J/kT}). \tag{6}$$

By comparing the relative intensities of the spin-1 ESR spectrum at 4.2 and 77 K, one can infer the value $J = 10 \pm 1$ cm^{-1} for the isotropic exchange interaction.

The curious temperature dependence of the spin-1 ESR spectrum, and the nature of its relation to the optical density of the 565-nm band, suggest that the 565-nm band produced by uv irradiation at 77 K may be associated with isolated spin-$\frac{1}{2}$ defects which subsequently aggregate during the fast-annealing stage to form exchange-coupled pairs. The optical-absorption spectrum of the exchange-coupled pairs is only slightly perturbed from that of the the isolated defects, which accounts for the altered appearance of the 565-nm band as shown in Fig. 10. The loss of intensity of the 565-nm band during the fast-annealing stage may simply reflect a small change in oscillator strength; alternatively, some defects may be lost in the process of aggregation. Ample precedent has been established for exchange-coupled pairs of trapped holes in the oxides,[15,16] and, in particular, a similar modification of an optical-absorption band has been observed in the analogous transformation from V^- to V^0 centers in MgO.[17]

The only spin-$\frac{1}{2}$ ESR spectrum which is observed to anneal during the fast-annealing stage of the 565-nm band is the broad single line on the high-field side in Fig. 2, whose intensity is not comparable with that of the spin-1 spectrum which replaces it. Thus an ESR spectrum corresponding to the isolated spin-$\frac{1}{2}$ defects which coalesce to form exchange-coupled pairs is not in evidence. One cannot argue conclusively from the absence of an ESR spectrum, since a deviant spin-lattice relaxation rate may render it unobservable; e.g., the ESR spectrum of isolated substitutional N_2^- in x-ray irradiated NaN_3 is invisible at 77 K.[9] Nevertheless an alternative model is suggested by the following considerations: Both isolated substitutional N_2^- ions[9] and nitrogen atoms[5] are produced by x-ray irradiation of NaN_3, presumably by the dissociation of single azide ions. Neither of these defects is produced in appreciable abundance by uv-irradiation at 77 K, which is consistent with the postulate that uv photolysis proceeds instead by a bimolecular reaction involving two adjacent azide ions. It seems probable that in some fraction of cases molecular fragments are left behind in the double anion vacancies thus formed in a plane perpendicular to the c axis; i.e., with the conformation shown in Fig. 9 of Ref. 1. The exchange coupling in this case would be much stronger than for the conformation shown in Fig. 11; an isotropic exchange interaction of several hundred cm^{-1} would leave the pair in a singlet state at all relevant temperatures, thus accounting for the absence of an ESR spectrum associated with an isolated spin-$\frac{1}{2}$ defect. In this alternative model, the appearance of the spin-1 ESR spectrum corresponds to a stage in the dissociation of exchange-coupled pairs, rather than to aggregation of isolated defects.

On either model, the 565-nm band is associated

with a component defect with $S=\frac{1}{2}$, but, in the absence of a corresponding ESR spectrum, we must rely on the spin-1 ESR spectrum (pair spectrum) for information about its properties. Since any hyperfine splitting must be accommodated within the observed linewidth of the pair spectrum (but with the hyperfine constants reduced by a factor of 2),[14] it seems probable that the component defect consists only of some combination of nitrogen atoms. Furthermore, its insensitivity to internal photoemission in "old" crystals,[1] and its propensity to aggregate, suggest that the defect is neutral with respect to the lattice. The precedent of exchange-coupled pairs of holes trapped at cation sites in the oxides suggests a similar model for the present defect. However, since a valence-band hole in NaN_3 can be described alternately as N_3 at an anion site, which has a π^3 ground configuration, its ESR spectrum should exhibit a positive g shift, contrary to what we observe in the pair spectrum. Other spin-$\frac{1}{2}$ molecular ions which have been detected in alkali azides by ESR include N_2^-,[9,18-20] N_4^-,[21] and N_3^{2-},[22,23] all of which have negative g shifts.

The 565-nm band in NaN_3 closely resembles a 565-nm band in uv-irradiated KN_3, which has been tentatively associated with N_2^- in an azide-ion vacancy. The molecular axes of the N_2^- ions in KN_3 are oriented perpendicular to the tetragonal c axis, and the 565-nm band is polarized perpendicular to the c axis, in contrast to the situation in NaN_3, where both the N_2^- molecular axis and the polarization of the 565-nm band are parallel to the hexagonal c axis. In KN_3, there is a thermally-activated transformation from N_2^- to N_4^- on warming to room temperature, which suggests aggregation of the N_2^- ions. Aggregates of N_2^- ions in NaN_3 could occur as exchange-coupled pairs instead. Substitutional N_2^-, which has the additional virtue that it is neutral with respect to the lattice, would provide the simplest model for the required spin-$\frac{1}{2}$ defect. Its ESR spectrum[9] is not observed even at 4.2 K in uv-irradiated NaN_3, but this could be explained by the alternative model of strongly exchange-coupled pairs. The N_2^- model has a number of additional difficulties, however. A very large crystal-field splitting of the degenerate π level, arising from lattice distortion associated with pair formation or off-center positions of the ions, would be required in order to produce as small a g shift as that observed in the spin-1 spectrum (−0.01).[24] The anion site has nearly axial symmetry, with the consequence that isolated substitutional N_2^- has a much larger g shift (−0.25).[9] Also, a molecular-orbital calculation with configuration interaction[25] for free N_2^- indicates that the $^2\Pi_u \leftarrow {}^2\Pi_g$ transition energy is closer to 4.8 eV than to 2.2 eV as required for the 565-nm band, and this conclusion appears to be supported by inelastic electron-scattering experiments.[26] Finally, a single crystal of NaN_3 was subjected to prolonged x-ray irradiation at room temperature to produce an intense N_2^- ESR spectrum[9] at 4.2 K, and it was established conclusively that no visible optical absorption with either polarization could be associated with this defect. (This observation would appear to rule out N_2^- as the source of the 565-nm band in KN_3 as well as in NaN_3.)

Substitutional N_4^- is also neutral with respect to the lattice, and the g values for its ESR spectrum[21] in KN_3 resemble those for the spin-1 spectrum in NaN_3. However, in contrast to the present defect, the principal axis associated with the greatest negative g shift in N_4^- is perpendicular to its transition moment for optical absorption,[27] which would appear to rule it out.

The remaining molecular ion, N_3^{2-}, is an interesting possibility. Its reported g values in[22] BaN_6 and[23] KN_3 are close to the free-electron value as a consequence of a bent ground-state configuration, and resemble those for the spin-1 spectrum in NaN_3. The long axis of the molecule would have to be perpendicular to the hexagonal c axis in NaN_3 in order to provide the observed g values. Conceivably, the N_3^{2-} ion occupies a pair of adjacent anion sites in a plane perpendicular to the c axis, which would make the defect neutral with respect to the lattice. The exchange-coupled pairs of defects would then involve a cluster of four anion sites. Unfortunately, the N_3^{2-} model is open to the same objection as the N_4^- model, in that its ESR spectrum in KN_3 (whose identification remains somewhat controversial)[28] reveals that the principal axis associated with the greatest negative g shift is parallel to the tetragonal c axis, and no optical absorption is detected with that polarization.[27]

Another spin-$\frac{1}{2}$ defect to be considered is cyclic N_3 which has been identified in NaN_3,[29] and KN_3,[30] on the basis of far-infrared spectra of isotopically enriched samples. However, the pulsed annealing of the cyclic N_3 infrared spectrum in NaN_3 was found to correlate with the 610-nm band rather than the 565-nm band.[31]

Inhomogeneous pairs such as N_3-N_3^{2-} or N_2^--N_4^- could also account for the spin-1 spectrum, with $\tilde{g}$ replaced by $\frac{1}{2}(\tilde{g}_1+\tilde{g}_2)$ in Eq. (3). However, these combinations are open to many of the same objections as the homogeneous pairs already considered.

In spite of the success of the point-ion model for the F_2^+ center, and the abundance of ESR spectra, it is now apparent that no spin-$\frac{1}{2}$ ESR spectrum has been observed which corresponds to this center.

However, as noted previously, one cannot argue conclusively from the absence of an ESR spectrum. The single, prominent ESR line in Fig. 2, which had previously been thought to correlate with the F_2^+ center,[6] remains to be identified. Its annealing behavior resembles that of the persistent component of the 735-nm band,[1] which may correspond to perturbed F centers, although its narrow linewidth is difficult to reconcile with such a model. This correlation is too imprecise for a conclusive identification at present.

In summary, the 565-nm band in uv-irradiated NaN_3 is associated with antiferromagnetically exchange-coupled pairs of spin-$\frac{1}{2}$ defects. None of the models considered for these component defects is entirely satisfactory. The prominent single ESR line does not correlate with the 610-nm band (F_2^+ center) as previously reported.[6] The 19-line F-center ESR spectrum correlates with the less-stable component of the 735-nm band.

ACKNOWLEDGMENTS

The authors are grateful to Professor O. R. Gilliam for providing NaN_3 crystals and to Dr. Maryn Stapelbroek and Robert Bossoli for assistance with x-ray orientation of crystals and with ESR measurements. We are also indebted to Professor B. S. H. Royce, Dr. David Welch, and Dr. Peter Kemmey for illuminating discussions.

*Supported by the U. S. Army Research Office, Durham, N. C. Grant No. DAHC04-75-G-0128.

[1]L. A. Kappers, P. K. Jain and R. H. Bartram, preceding paper, Phys. Rev. B 14, 5473 (1976).

[2]G. J. King, B. S. Miller, F. F. Carlson, and R. C. McMillan, J. Chem. Phys. 32, 940 (1960).

[3]B. S. Miller, J. Chem. Phys. 33, 889 (1960).

[4]F. F. Carlson, G. J. King, and B. S. Miller, J. Chem. Phys. 33, 1266 (1960).

[5]G. J. King, F. F. Carlson, B. S. Miller, and R. C. McMillan, J. Chem. Phys. 34, 1499 (1961).

[6]G. J. King, B. S. Miller, F. F. Carlson, and R. C. McMillan, J. Chem. Phys. 35, 1442 (1961).

[7]F. F. Carlson, J. Chem. Phys. 39, 1206 (1961).

[8]B. S. Miller, J. Chem. Phys. 40, 2371 (1964).

[9]E. Gelerinter and R. H. Silsbee, J. Chem. Phys. 45, 1703 (1966).

[10]G. W. Brezina and E. Gelerinter, J. Chem. Phys. 49, 3293 (1968).

[11]E. Gelerinter, J. Chem. Phys. 53, 2991 (1970).

[12]R. H. Bartram and L. A. Kappers, Bull. Am. Phys. Soc. 21, 780 (1976).

[13]G. E. Pringle and D. E. Noakes, Acta Crystallogr. B 24, 262 (1968).

[14]J. Owen, J. Appl. Phys. Suppl. 32, 213S (1961).

[15]A. E. Hughes and B. Henderson, in *Point Defects in Ionic Crystals*, edited by J. H. Crawford, Jr. and L. M. Slifkin (Plenum, New York, 1972), Vol. 1, pp. 381–490.

[16]A. M. Stoneham, A. P. Pathak, and R. H. Bartram, J. Phys. C 9, 73 (1976).

[17]L. A. Kappers, F. Dravnieks, and J. E. Wertz, J. Phys. C 7, 1387 (1974).

[18]D. W. Wylie, A. J. Shuskus, C. G. Young, O. R. Gilliam, and P. W. Levy, Phys. Rev. 125, 451 (1962).

[19]R. B. Horst, J. H. Anderson, and D. E. Milligan, J. Phys. Chem. Solids 23, 157 (1962).

[20]P. L. Marinkas and R. H. Bartram, J. Chem. Phys. 48, 927 (1968).

[21]A. J. Shuskus, C. G. Young, O. R. Gilliam, and P. W. Levy, J. Chem. Phys. 33, 622 (1960).

[22]P. L. Marinkas, J. Chem. Phys. 52, 5144 (1970).

[23]G. W. Neilson and M. C. R. Symons, J. Chem. Soc. Faraday II 68, 1772 (1972).

[24]R. H. Bartram, C. R. Fischer, and P. J. Kemmey, Phys. Rev. B 9, 1777 (1974).

[25]E. W. Thulstrup and A. Andersen, J. Phys. B 8, 965 (1975).

[26]J. Mazeau, F. Grestau, R. I. Hall, G. Joyez, and J. Reinhardt, J. Phys. B 6, 862 (1973).

[27]L. D. Bogan, R. H. Bartram, and F. J. Owens, Phys. Rev. B 6, 3090 (1972).

[28]F. J. Owens, Phys. Lett. 33A, 41 (1970).

[29]J. I. Bryant, J. Chem. Phys. 42, 2270 (1965).

[30]J. I. Bryant, Spectrochim. Acta 22, 1475 (1966).

[31]H. A. Papazian, J. Phys. Chem. Solids 21, 81 (1961).